

1.8-kV circular AlGaN/GaN/AlGaN double-heterostructure high electron mobility transistor

Sheng-Lei Zhao(赵胜雷), Zhi-Zhe Wang(王之哲), Da-Zheng Chen(陈大正), Mao-Jun Wang(王茂俊), Yang Dai(戴扬), Xiao-Hua Ma(马晓华), Jin-Cheng Zhang(张进成), Yue Hao(郝跃)

Citation: Chin. Phys. B . 2019, 28(2): 027301. **doi:** 10.1088/1674-1056/28/2/027301
Journal homepage: http://cpb.iphy.ac.cn; http://iopscience.iop.org/cpb

What follows is a list of articles you may be interested in

Low specific on-resistance GaN-based vertical heterostructure field effect transistors with nonuniform doping superjunctions

Wei Mao(毛维), Hai-Yong Wang(王海永), Peng-Hao Shi(石朋毫), Xiao-Fei Wang(王晓飞), Ming Du(杜鸣), Xue-Feng Zheng(郑雪峰), Chong Wang(王冲), Xiao-Hua Ma(马晓华), Jin-Cheng Zhang(张进成), Yue Hao(郝跃)

Chin. Phys. B . 2018, 27(4): 047305. **doi:** 10.1088/1674-1056/27/4/047305

Analysis of the modulation mechanisms of the electric field and breakdown performance in AlGaN/GaN HEMT with a T-shaped field-plate

Wei Mao(毛维), Ju-Sheng Fan(范举胜), Ming Du(杜鸣), Jin-Feng Zhang(张金凤), Xue-Feng Zheng(郑雪峰), Chong Wang(王冲), Xiao-Hua Ma(马晓华), Jin-Cheng Zhang(张进成), Yue Hao(郝跃)

Chin. Phys. B . 2016, 25(12): 127305. **doi:** 10.1088/1674-1056/25/12/127305

A uniform doping ultra-thin SOI LDMOS with accumulation-mode extended gate and back-side etching technology

Yan-Hui Zhang(张彦辉), Jie Wei(魏杰), Chao Yin(尹超), Qiao Tan(谭桥), Jian-Ping Liu(刘建平), Peng-Cheng Li(李鹏程), Xiao-Rong Luo(罗小蓉)

Chin. Phys. B . 2016, 25(2): 027306. **doi:** 10.1088/1674-1056/25/2/027306

Effect of gate length on breakdown voltage in AlGaN/GaN high-electron-mobility transistor

Jun Luo(罗俊), Sheng-Lei Zhao(赵胜雷), Min-Han Mi(宓珉瀚), Wei-Wei Chen(陈伟伟), Bin Hou(侯斌), Jin-Cheng Zhang(张进成), Xiao-Hua Ma(马晓华), Yue Hao(郝跃)

Chin. Phys. B . 2016, 25(2): 027303. **doi:** 10.1088/1674-1056/25/2/027303

Reverse blocking characteristics and mechanisms in Schottky-drainAlGaN/GaN HEMT with a drain field plate and floating field plates

Wei Mao(毛维), Wei-Bo She(佘伟波), Cui Yang(杨翠), Jin-Feng Zhang(张金凤), Xue-Feng Zheng(郑雪峰), Chong Wang(王冲), Yue Hao(郝跃)

Chin. Phys. B . 2016, 25(1): 017303. **doi:** 10.1088/1674-1056/25/1/017303

1.8-kV circular AlGaN/GaN/AlGaN double-heterostructure high electron mobility transistor*

Sheng-Lei Zhao(赵胜雷)[1], Zhi-Zhe Wang(王之哲)[2], Da-Zheng Chen(陈大正)[1], Mao-Jun Wang(王茂俊)[3], Yang Dai(戴扬)[4], Xiao-Hua Ma(马晓华)[1], Jin-Cheng Zhang(张进成)[1,†], and Yue Hao(郝跃)[1]

[1] *Key Laboratory for Wide Band-Gap Semiconductor Materials and Devices, School of Microelectronics, Xidian University, Xi'an* 710071, *China*

[2] *China Electronic Product Reliability and Environmental Testing Research Institute, Guangzhou* 510610, *China*

[3] *Institute of Microelectronics, Peking University, Beijing* 100871, *China*

[4] *School of Information Science and Technology, Northwest University, Xi'an* 710127, *China*

(Received 5 September 2018; revised manuscript received 27 November 2018; published online 10 January 2019)

In this paper, we present a 1.8-kV circular AlGaN/GaN/AlGaN double-heterostructure high electron mobility transistor (DH HEMT) with a gate-drain spacing $L_{GD} = 18.8$ μm. Compared with the regular DH HEMT, our circular structure has a high average breakdown electric-field strength that increases from 0.42 MV/cm to 0.96 MV/cm. The power figure of merit V_{BR}^2/R_{ON} for the circular HEMT is as high as 1.03×10^9 $V^2\cdot\Omega^{-1}\cdot cm^{-2}$. The divergence of electric field lines at the gate edge and no edge effect account for the breakdown enhancement capability of the circular structure. Experiments and analysis indicate that the circular structure is an effective method to modulate the electric field.

Keywords: AlGaN/GaN/AlGaN DH HEMTs, circular structure, breakdown voltage

PACS: 73.40.Kp, 73.61.Ey, 78.30.Fs **DOI:** 10.1088/1674-1056/28/2/027301

1. Introduction

GaN-based high electron mobility transistors (HEMTs) are excellent candidates for power electronic applications due to excellent material and device properties, such as high breakdown voltage (V_{BR}) and low specific on-resistance (R_{ON}).[1–6] Breakdown voltage is a very important parameter for power electronic devices. Although numerous studies on improving V_{BR} have been carried out and excellent breakdown performances have been achieved, the breakdown voltages of GaN-based HEMTs are still far from their theoretical performance limit. For GaN-based HEMTs, there exists a high electric field at the drain-side edge of the gate terminal, which restricts the achievement of high V_{BR}. In order to reduce the high electric field, various field plates (FPs) were introduced, including gate FP, source FP, and slant FP.[7,8] The electric field peak was reduced effectively by the introduction of FPs, which improves V_{BR} significantly. In addition, double heterostructure (DH) HEMTs were utilized to reduce the buffer leakage current and improve breakdown characteristics.[9]

In this paper, we present another technique to modulate the electric field, namely circular structure. The reported GaN-based HEMTs in previous studies are almost fabricated based on bar-type structure.[10,11] This regular and circular AlGaN/GaN/AlGaN DH HEMTs are fabricated and compared on the same wafer. A high breakdown voltage of 1812 V is achieved for the circular AlGaN/GaN HEMT with a gate–drain spacing $L_{GD} = 18.8$ μm. The average breakdown electric-field strength is increased from 0.42 MV/cm for regular HEMT to 0.96 MV/cm for circular HEMT. Besides, the electric-field modulation of the circular structure is explained through two aspects.

2. Device fabrication

Figure 1 shows the schematic diagram of the circular AlGaN/GaN/AlGaN DH HEMT. The heterojunction structure was grown on a sapphire substrate by metal-organic chemical vapor deposition. The buffer layer contained a 0.75-μm GaN layer and a 0.75-μm linearly graded $Al_xGa_{1-x}N$ layer with Al maximum content of 7% from the interface to a 15-nm GaN channel layer. The AlGaN buffer layer acted as a back barrier layer, which can reduce the buffer leakage current.[9] As shown in Fig. 2, the conduction band diagrams and electron distributions for conventional AlGaN back barrier and linearly graded AlGaN back barrier were calculated by self-consistently solving a one-dimensional (1D) Poisson–Schrödinger equation. For conventional AlGaN back barrier, a secondary channel at the interface of conventional-AlGaN/GaN buffer layers could be produced by polarization-induced doping. In contrast, the polarization at the interface of graded-AlGaN/GaN buffer layers was very weak, and the secondary channel could be removed. The 1-nm AlN interlayer was grown to improve two-dimensional (2D) electron gas

*Project supported by the National Key Research and Development Program of China (Grant No. 2016YFB0400100), the National Natural Science Foundation of China (Grant Nos. 11435010, 61474086, and 61804125), and the Natural Science Basic Research Program of Shaanxi Province, China (Grant No. 2016ZDJC-02).

†Corresponding author. E-mail: jchzhang@xidian.edu.cn

© 2019 Chinese Physical Society and IOP Publishing Ltd

(2DEG) mobility, followed by growing a 21-nm $Al_{0.3}Ga_{0.7}N$ barrier layer and a 1.5-nm GaN cap layer. Hall measurements showed a sheet carrier density of 8.6×10^{12} cm^{-2}, a 2DEG mobility of 1739 cm^2/V·s, and a sheet resistance of 417 Ω/sq. The device fabrication started with mesa isolation by reactive ion etching (RIE) using Cl_2 plasma. Ohmic metal was formed by using Ti/Al/Ni/Au, and Schottky gate was formed by using Ni/Au/Ni layers.

As shown in Fig. 1(b), the drain electrode had a round structure, and it was arranged in the center of the device with a radius $R_1 = 68$ μm. The gate and source electrodes both had a circular structure. The tested circular HEMT had a gate-drain spacing $L_{GD} = 18.8$ μm, a gate length $L_G = 0.8$ μm, a gate–source spacing $L_{GS} = 1.4$ μm, and a source contact length $L_{source} = 34$ μm. The drain-side FP of the T-shape gate had a length of 0.8 μm. The distance from the drain center to gate was $R_2 = 86.8$ μm. To investigate the influence of the circular structure, we measured the breakdown characteristics of the regular devices with $L_{GD} = 1.6$ μm, 2.6 μm, 3.6 μm, and 10 μm on the same wafer.

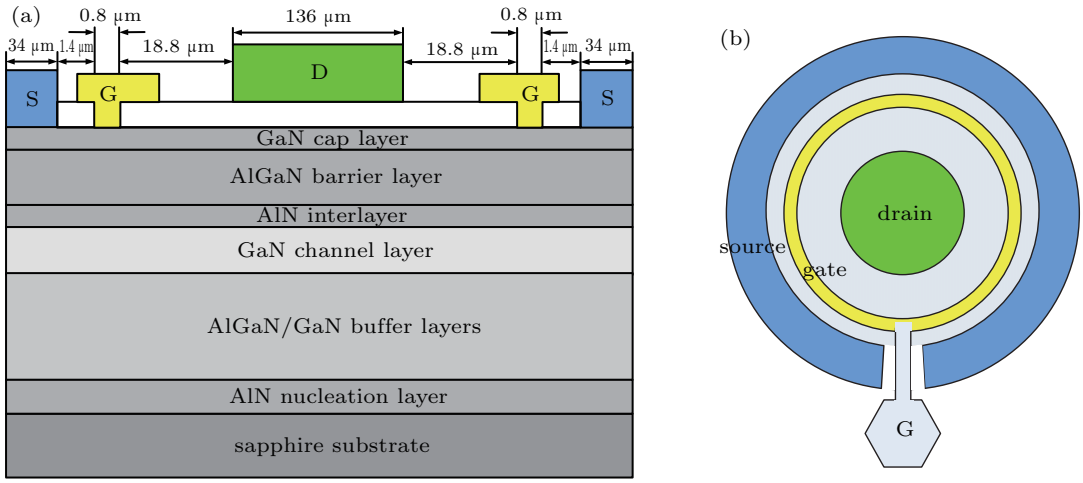


Fig. 1. (a) Cross-sectional view and (b) top view of circular AlGaN/GaN/AlGaN DH HEMT.

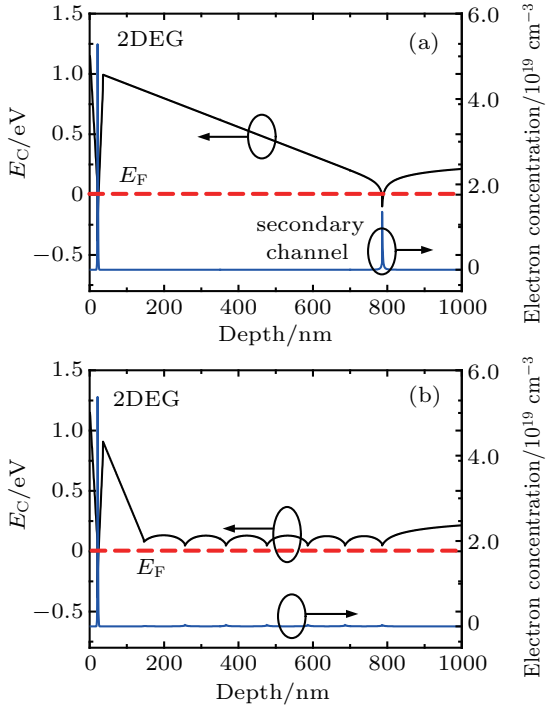


Fig. 2. Calculated conduction band diagrams and electron distributions for (a) conventional AlGaN back barrier and (b) linearly graded AlGaN back barrier. Al content in AlGaN barrier layer is 7%.

3. Results and discussion

The output characteristics of the regular and circular AlGaN/GaN/AlGaN DH HEMTs are shown in Fig. 3(a). For the regular HEMT with $L_{GD} = 10$ μm and the circular HEMT with $L_{GD} = 18.8$ μm, the maximum drain currents are 634 mA/mm and 360 mA/mm, respectively. The specific on-resistance R_{ON} is the product of on-resistance R_{on} and the device active area A, with considering a 1.5-μm transfer length of the ohmic contact. The on-resistance R_{on} can be extracted from the output curves. The value of R_{ON} of the circular HEMT is 3.19 mΩ·cm^2, which is larger than that of the regular HEMT (0.91 mΩ·cm^2) due to larger L_{GD} and the circular structure. Figure 3(b) shows the transfer characteristics of the circular HEMT. The threshold voltage is −2.5 V, and the maximum transconductance is 140 mS/mm.

With gate biased at −6 V, the breakdown characteristics of the regular and circular HEMT are measured as shown in Fig. 4(a). The breakdown measurements were carried out with devices immersed in Fluorinert to prevent surface flashover, and the breakdown criterion of the HEMT is 1 mA/mm.

The breakdown voltages of the regular HEMTs with $L_{GD} = 1.6$ μm, 2.6 μm, 3.6 μm, and 10 μm are 66 V, 106 V, 154 V, and 423 V, respectively. As shown in Fig. 4(b), the average breakdown electric-field strength E_{BR} of the regular HEMT is 0.42 MV/cm. The value of V_{BR} of the circular HEMT with $L_{GD} = 18.8$ μm is 1812 V, indicating that the E_{BR} of the circular HEMT is 0.96 MV/cm. The circular HEMT demonstrates a 128.6% improvement of E_{BR} compared with the regular HEMT.

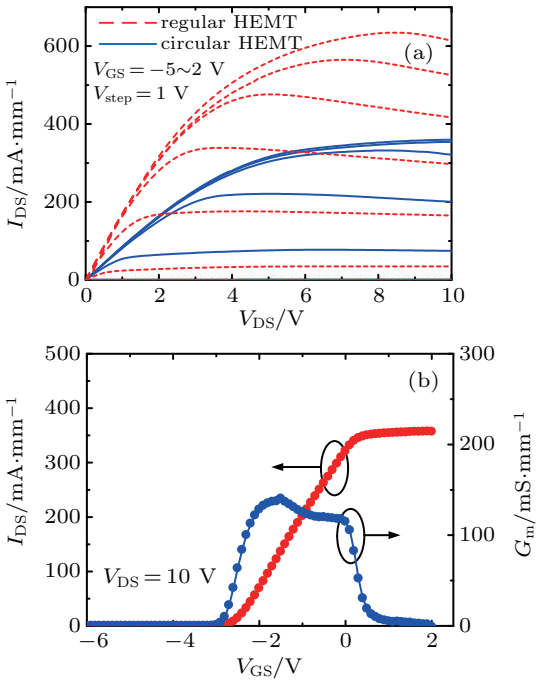


Fig. 3. (a) Output characteristics of regular HEMT with $L_{GD} = 10$ μm and circular HEMT with $L_{GD} = 18.8$ μm. (b) Transfer characteristics of circular HEMT with $L_{GD} = 18.8$ μm.

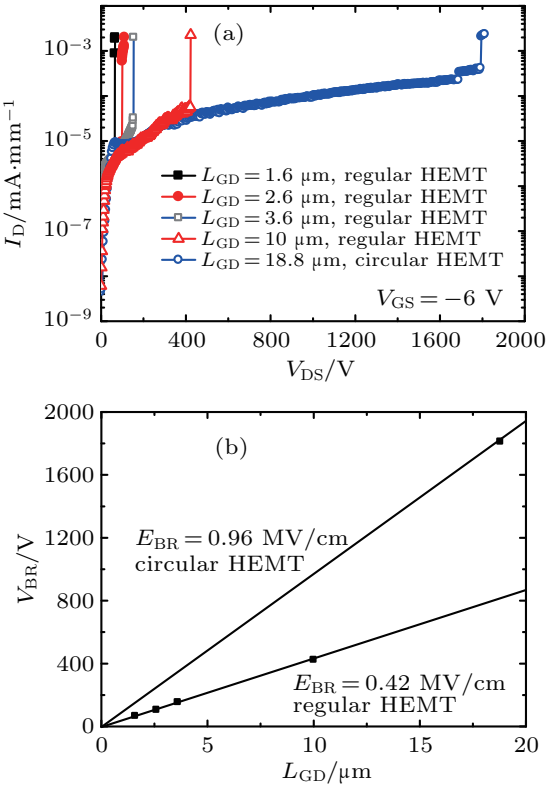


Fig. 4. (a) Breakdown characteristics of regular and circular DH HEMTs. (b) Off-state breakdown voltage V_{BR} versus gate-drain spacing L_{GD}.

The power figure of merit V_{BR}^2/R_{ON} for the regular HMET with $L_{GD} = 10$ μm is 1.97×10^8 V$^2 \cdot \Omega^{-1}$·cm^{-2}. In contrast, V_{BR}^2/R_{ON} for the circular HEMT with $L_{GD} = 18.8$ μm is as high as 1.03×10^9 V$^2 \cdot \Omega^{-1}$·cm^{-2}, which is one of the best values ever reported for GaN-based HEMTs.[12–14]

The actual electric-field line distributions in GaN-based HEMTs are very complicated. In the fabricated GaN-based HEMT, a high electric field exists at the drain-side edge of the gate terminal due to the formation of the depletion region near the gate. In order to explain the breakdown enhancement capability of the circular structure, the schematic electric-field line distribution of regular and circular HEMTs are drawn in Fig. 5. During breakdown measurements, electric-field lines point from drain to gate. Due to the divergence of electric field lines, the electric field at the gate edge (point B) of the circular structure can be reduced compared with that of the regular structure. In addition, there is no end of the gate (point C) for the circular HEMT, and the circular structure can avoid such an edge effect. These two reasons account for the breakdown enhancement capability of the circular structure.

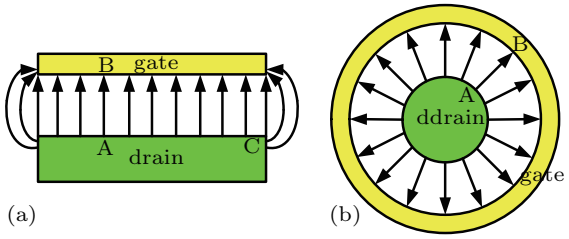


Fig. 5. Schematic electric-field line distributions of (a) regular and (b) circular HEMTs.

With the decrease of the drain electrode radius, electric field of point B decreases and electric field at point A increases. The breakdown voltage may be improved with the drain electrode radius decreasing. When the drain electrode radius is very small, electric field at point A is very high, and breakdown voltage decreases. Thus, a very high breakdown voltage can be achieved by optimizing the drain electrode radius.

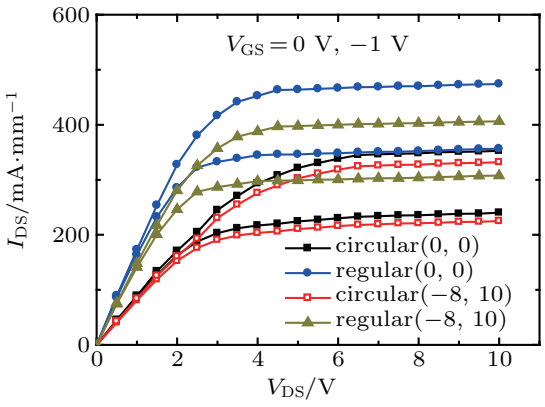


Fig. 6. Pulsed *I*–*V* characteristics of regular and circular HEMTs.

The pulsed *I*–*V* characteristics are measured to characterize the DC-to-RF dispersion in the two HEMTs. The pulse width and pulse period are 500 ns and 1 ms, respectively. As shown in Fig. 6, compared with the pulsed currents at the bias point $(V_{GSQ}, V_{DSQ}) = (0, 0)$, those at $(V_{GSQ}, V_{DSQ}) = (-8, 10)$ of the regular and circular HEMTs are reduced by 14% and 6% respectively at $V_{GS} = 0$ V and $V_{DS} = 10$ V. Therefore, the

dynamic characteristics of the circular HEMT are improved through the reduction of the electric field at the gate edge.

4. Conclusions

A 1.8-kV circular AlGaN/GaN/AlGaN DH HEMT is presented in this paper. The circular DH HEMT demonstrates a 128.6% improvement of E_{BR} compared with the regular DH HEMT. The power figure of merit V_{BR}^2/R_{ON} can be improved from 1.97×10^8 $V^2 \cdot \Omega^{-1} \cdot cm^{-2}$ to 1.03×10^9 $V^2 \cdot \Omega^{-1} \cdot cm^{-2}$. By optimizing the drain electrode radius, the electric-field distribution is more even and breakdown voltage is higher. The circular structure proves to be an effective method to modulate electric field as field plates, and it also very promising to have applications in power electronics.

References

[1] Tipirneni N, Koudymov A, Adivarahan V, Yang J, Simin G and Khan M A 2006 *IEEE Electron Dev. Lett.* **27** 716

[2] Selvaraj S L, Suzue T and Egawa T 2009 *IEEE Electron Dev. Lett.* **30** 587

[3] Zhao S L, Hou B, Chen W W, Mi M H, Zheng J X, Zhang J C, Ma X H and Hao Y 2016 *IEEE Trans. Power Electron.* **31** 1517

[4] Xiao M, Duan X L, Zhang J C and Hao Y 2018 *IEEE Electron Dev. Lett.* **39** 719

[5] Liu T T, Zhang K, Zhu G R, Zhou J J, Kong Y C, Yu X X and Chen T S 2018 *Chin. Phys. B* **27** 047307

[6] Han T C, Zhao H D, Yang L and Wang Y 2017 *Chin. Phys. B* **26** 107301

[7] Karmalkar S and Mishra U K 2001 *IEEE Trans. Electron. Dev.* **48** 1515

[8] Xing H L, Dora Y, Chini A, Heikman S, Keller S and Mishra U K 2004 *IEEE Electron Dev. Lett.* **25** 161

[9] Treidel E B, Hilt O, Brunner F, Würfl J and Tränkle G 2008 *IEEE Trans. Electron. Dev.* **55** 3354

[10] Yang S, Huang S, Chen H, Zhou C, Zhou Q, Schnee M, Zhao Q T, Schubert J and Chen K J 2012 *IEEE Electron Dev. Lett.* **33** 979

[11] Meneghini M, Cibin G, Bertin M, Hurkx G A M, Šonský P I J, Croon J A, Meneghesso G and Zanoni E 2014 *IEEE Trans. Electron. Dev.* **61** 1987

[12] Treidel E B, Brunner F, Hilt O, Cho E, Würfl J and Tränkle G 2010 *IEEE Trans. Electron. Dev.* **57** 3050

[13] Selvaraj S L, Watanabe A, Wakejima A and Egawa T 2012 *IEEE Electron Dev. Lett.* **33** 1375

[14] Lee H S, Piedra D, Sun M, Gao X, Guo S and Palacios T 2012 *IEEE Electron Dev. Lett.* **33** 982